

Supporting Information

Synthesis, Properties, and OLED Characteristics of 2,2'-Bipyridine-Based Electron-Transporters: Synergistic Effect of Molecular Shape Anisotropy and Weak Hydrogen Bonding Network on Molecular Orientation

Yuichiro Watanabe,^[a] Hisahiro Sasabe,^{,[a],[b]} Daisuke Yokoyama,^{[a],[b]} Teruo Beppu,^[a] Hiroshi Katagiri,^{[a],[b]} and Junji Kido^{*,[a],[b]}*

[a] Department of Organic Device Engineering, Graduate School of Science and Engineering, Yamagata University, Yonezawa, Yamagata, 992-8510 Japan.

[b] Research Center for Organic Electronics (ROEL), Yamagata University, Yonezawa, Yamagata, 992-8510 Japan.

E-mail: h-sasabe@yz.yamagata-u.ac.jp; kid@yz.yamagata-u.ac.jp

Table of Contents:

- 1. Experimental section**
- 2. DFT Calculations**
- 3. Synthesis**
- 4. X-Ray Crystal Structure Determination**
- 5. Thermal Properties**
- 6. Optical Properties**
- 7. Time of Flight Measurement**
- 8. Electron Only Devices**
- 9. Organic Light Emitting Devices (OLEDs)**
- 10. References**

1. Experimental Section

General considerations: Quantum chemical calculations were performed using the hybrid density functional theory (DFT) functional Becke and Hartree-Fock exchange and Lee Yang and Parr correlation (B3LYP) as implemented by the Gaussian 09 program packages.^[1] Electrons were described by the Pople's 6-31G(d,p) and 6-311 + G(d,p) basis sets for molecular structure optimization and single-point energy calculations, respectively. ¹H NMR spectrum was recorded on JEOL 400 (400 MHz) spectrometer. Mass spectrum was obtained using a JEOL JMS-K9 mass spectrometer. Differential scanning calorimetry (DSC) was performed using a Perkin-Elmer Diamond DSC Pyris instrument under nitrogen atmosphere at a heating rate of 10°C min⁻¹. Thermogravimetric analysis (TGA) was undertaken using a SEIKO EXSTAR 6000 TG/DTA 6200 unit under nitrogen atmosphere at a heating rate of 10°C min⁻¹. UV-Vis spectra were measured using a Shimadzu UV-3150 UV-vis-NIR spectrophotometer. Photoluminescence spectra were measured using a FluroMax-2 (Jobin-Yvon-Spex) luminescence spectrometer. The ionization potential (I_p) was determined by a photoelectron yield spectroscopy (PYS) under the vacuum ($\sim 10^{-3}$ Pa). The deposited films for PYS measurement were transported through in nitrogen globe box without atmospherically exposed.

Device Fabrication and Characterization: CBP and Liq were purchased from eRay. TAPC was purchased from TCI. Ir(ppy)₃ was purchased from Chemipro Kasei. CBP and TAPC were purified by temperature-gradient sublimation in vacuum. Phosphorescent OLEDs were grown on glass substrates precoated with a 130-nm thick layer of indium-tin oxide (ITO) having a sheet resistance of 15 Ω/sq. The substrates

were cleaned with ultrapurified water and organic solvents, and then dry-cleaned for 30 min by exposure to UV–ozone. The organic layers were deposited onto the ITO substrate under the vacuum (ca. 10^{-5} Pa), successively. Al was patterned using a shadow mask with an array of 2 mm \times 2 mm openings without breaking the vacuum (ca. 10^{-5} Pa). All devices were encapsulated immediately after preparation under a nitrogen atmosphere using epoxy glue and glass lids. The EL spectra were taken using an optical multichannel analyzer Hamamatsu Photonics PMA-11. The current density–voltage and luminance–voltage characteristics were measured using a Keithley source measure unit 2400 and a Minolta CS200 luminance meter, respectively.

2. Quantum chemical calculation

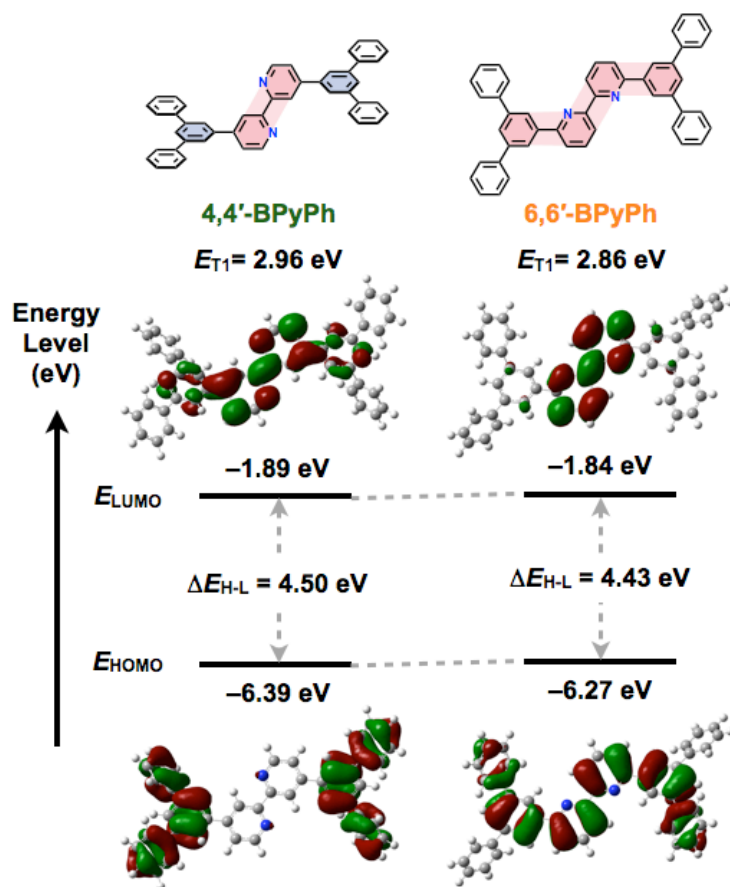


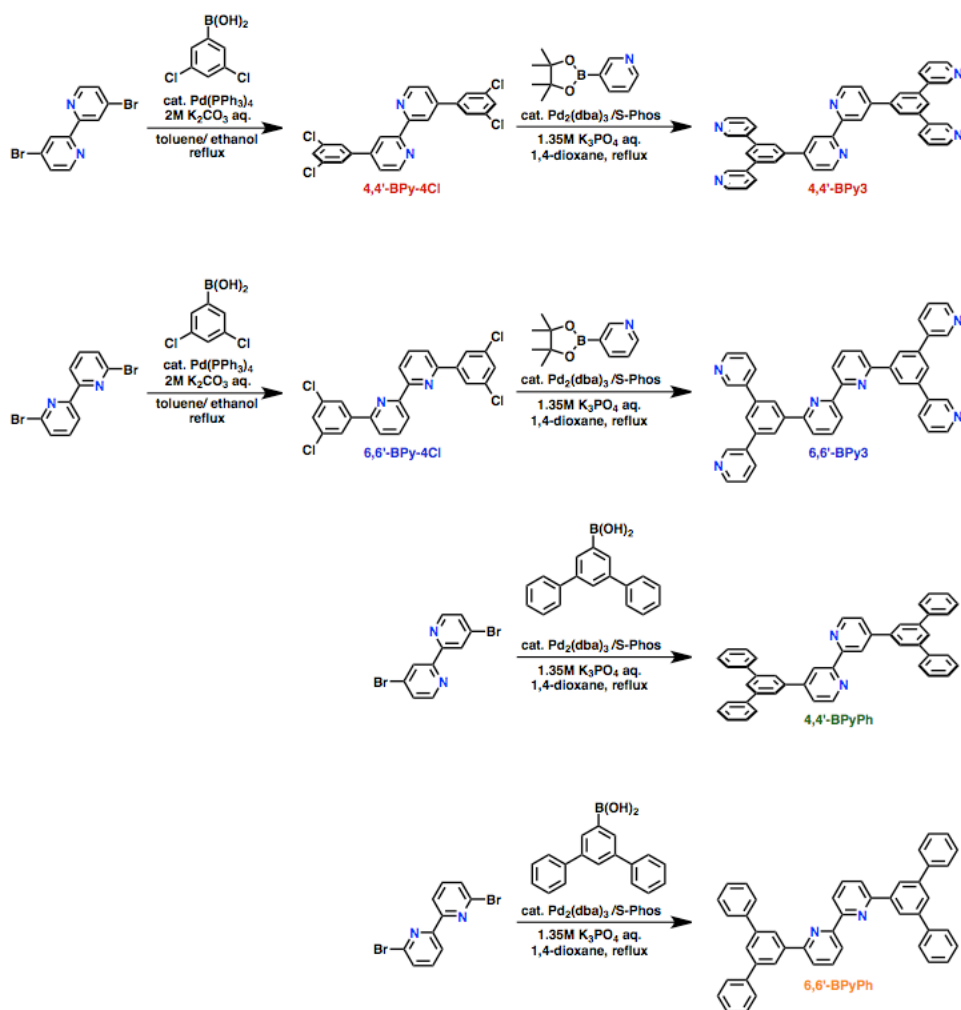
Figure S1. The calculated spatial distributions of HOMO and LUMO for BPyPh derivatives at the B3LYP 6-311+G(d,p)//6-31G(d,p) level.

Table S1. Calculated HOMO, LUMO, ΔE_{H-L} , E_S , E_T and ΔE_{ST} values (eV).

Compound	HOMO ^{a)}	LUMO ^{a)}	ΔE_{H-L} ^{b)}	E_S ^{c)}	E_T ^{d)}	ΔE_{ST} ^{d)}
4,4'-BPy3	-6.79	-2.10	4.69	3.62	2.96	0.66
6,6'-BPy3	-6.51	-2.01	4.50	3.45	2.86	0.59
4,4'-BPyPh	-6.39	-1.89	4.50	3.57	2.96	0.61
6,6'-BPyPh	-6.27	-1.84	4.43	3.95	2.86	1.09
TPBi	-6.00	-1.68	4.32	3.49	2.77	0.72

^{a)} Calculated at RB3LYP 6-311+G(d,p)//RB3LYP 6-31G(d). ^{b)} $\Delta E_{H-L} = \text{HOMO} - \text{LUMO}$. ^{c)} Lowest singlet (E_S) and triplet (E_T) energy from TD-DFT at RB3LYP 6-31G(d)//RB3LYP 6-31G(d). ^{d)} Energy difference between lowest singlet (E_S) and triplet (E_T) energy ($\Delta E_{ST} = E_S - E_T$).

3. Synthesis



Scheme S1. Synthetic route of BPy and BPyPh derivatives.

Synthesis of 4,4'-BPy-4Cl. 3,5-Dichlorophenyl boronic acid (3.87 g, 20.3 mmol) and 4,4'-Dibromo-2,2'-bipyridyl (3.14 g, 10.0 mmol) were added to a round bottom flask. Toluene (80 mL), ethanol (40 mL) and aqueous K₂CO₃ (2 M, 40 mL) were added and nitrogen (N₂) bubbled through the mixture for 1.5 hour. Then, Pd(PPh₃)₄ (0.29 g, 0.25 mmol) was added and the resultant mixture was stirred for 43 hours at reflux under N₂ flow. The precipitate was filtered, and washed with water and methanol. The resulting off-white solid was dissolved in reflux toluene 700 mL, filtered through silica-gel pad (200 cc) and washed with toluene. After the clear filtrate was concentrated to 50 mL, the precipitate was collected, washed with methanol, dried in vacuo to afford 4,4'-BPy-4Cl (2.67 g, 60%) as a white solid: Thin layer Chromatography (TLC) analysis, retention factor (*R_f*): 0.38 (eluent: chloroform/methanol = 20:1 v/v). ¹H NMR (400 MHz, Chloroform-d): δ = 8.79 (d, *J* = 5.0 Hz, 2H), 8.68 (d, *J* = 1.8 Hz, 2H), 7.66 (d, *J* = 1.8 Hz, 4H), 7.52 (dd, *J* = 5.2, 2.0 Hz, 2H), 7.46 (t, *J* = 1.8 Hz, 2H) ppm; EI-MS: *m/z* 447 [*M*+H]⁺.

Synthesis of 6,6'-BPy-4Cl. off white solid (41% yield). TLC analysis, *R_f*: 0.93 (eluent: chloroform/methanol = 20:1 v/v). ¹H NMR (400 MHz, Chloroform-d): δ = 8.62 (d, *J* = 7.8 Hz, 2H), 8.05 (d, *J* = 1.8 Hz, 4H), 7.98 (t, *J* = 8.0 Hz, 2H), 7.77 (d, *J* = 7.8 Hz, 2H), 7.44 (t, *J* = 1.8 Hz, 2H) ppm; EI-MS: *m/z* 447 [*M*+H]⁺.

Synthesis of 4,4'-BPy3. 3-(4,4,5,5-Tetramethyl-1,3,2-dioxaborolan-2-yl)pyridine (3.09 g, 15.0 mmol) and 4,4'-BPy-4Cl (1.34 g, 3.00 mmol) were added to a round bottom flask. 1,4-Dioxane (45 mL) and aqueous K₃PO₄ (1.35 M, 15 mL) were added and nitrogen bubbled through the mixture for 1 hour. Then, Pd₂(dba)₃ (0.057 g, 0.061 mmol) and 2-dicyclohexylphosphino-2',6'-dimethoxybiphenyl (S-Phos) (0.053 g, 0.13 mmol) were added and the resultant mixture was vigorously stirred for 51 hours at reflux temperature under N₂ flow. The precipitate was filtered, and washed with water and methanol. The resulting off-white solid was purified by chromatography on silica gel (eluent: CHCl₃/CH₃OH = 100:3, 100:5 to 100:10 v/v) to afford 4,4'-BPy3 (1.52 g, 82%) as a off white solid. TLC analysis, *R_f*: 0.15 (eluent: chloroform/methanol = 20:1 v/v). ¹H NMR (400 MHz, Chloroform-d): δ = 9.00 (d, *J* = 2.7 Hz, 4H), 8.90–8.80 (m, 4H), 8.70 (dd, *J* = 1.6, 5.2 Hz, 4H), 8.08–7.97 (m, 8H), 7.86 (t, *J* = 1.4 Hz, 2H), 7.69 (dd, *J* = 4.8, 1.6 Hz, 2H), 7.46 (dd, *J* = 8.0, 4.8 Hz, 4H) ppm; EI-MS: *m/z* 617 [*M*+H]⁺. Anal calcd for C₄₂H₂₈N₆: C, 81.80; H, 4.58; N, 13.63%. Found. C, 81.87; H, 4.45; N, 13.68%.

Synthesis of 6,6'-BPy3. off white solid (92% yield). TLC analysis, *R_f*: 0.23 (eluent: chloroform/methanol = 20:1 v/v). ¹H NMR (400 MHz, Chloroform-d): δ = 9.04 (d, *J* = 2.3 Hz, 4H), 8.77–8.64 (m, 6H), 8.42 (d, *J* = 1.8 Hz, 4H), 8.11–7.98 (m, 6H), 7.94 (d, *J* = 7.8 Hz, 2H), 7.85 (t, *J* = 1.6 Hz, 2H), 7.52–7.42 (m, 4H) ppm; EI-MS: *m/z* 617 [*M*+H]⁺. Anal calcd for C₄₂H₂₈N₆: C, 81.80; H, 4.58; N, 13.63%. Found. C, 82.01; H, 4.41; N, 13.62%.

Synthesis of 4,4'-BPyPh. 5'-*m*-Terphenylboronic acid (1.32 g, 4.8 mmol) and 4,4'-Dibromo-2,2'-bipyridyl (1.23 g, 2.0 mmol) were added to a round bottom flask. 1,4-Dioxane (30 mL) and aqueous K₃PO₄ (1.35 M, 10 mL) were added and nitrogen bubbled through the mixture for 1 hour. Then, Pd₂(dba)₃ (0.038 g, 0.041 mmol) and 2-dicyclohexylphosphino-2',6'-dimethoxybiphenyl (S-Phos) (0.034 g, 0.083 mmol) were

added and the resultant mixture was vigorously stirred for 13 hours at reflux temperature under N₂ flow. The precipitate was filtered, and washed with water and methanol. The resulting pale-yellow solid was dissolved in reflux toluene 500 mL, filtered through silica-gel pad (200 cc) and washed with toluene. The clear filtrate was further purified by recrystallization from toluene to afford 4,4'-BPy-4Cl (0.57 g, 46%) as a pale-yellow solid. TLC analysis, *R_f*: 0.35 (eluent: chloroform/methanol = 20:1 v/v). ¹H NMR (400 MHz, Chloroform-d) δ = 8.84 (d, *J* = 1.4 Hz, 2H), 8.80 (d, *J* = 5.0 Hz, 2H), 7.96 (d, *J* = 1.8 Hz, 5H), 7.89 (t, *J* = 1.6 Hz, 2H), 7.78–7.71 (m, 8H), 7.68 (dd, *J* = 5.2, 2.0 Hz, 2H), 7.56–7.46 (m, 8H), 7.46–7.38 (m, 4H) ppm; EI-MS: *m/z* 612 [*M*]⁺. Anal calcd for C₄₆H₃₂N₂: C, 90.16; H, 5.26; N, 4.57%. Found. C, 90.14; H, 5.26; N, 4.49%.

Synthesis of 6,6'-BPyPh. 5'-*m*-Terphenylboronic acid (1.32 g, 4.8 mmol) and 6,6'-Dibromo-2,2'-bipyridyl (1.23 g, 2.0 mmol) were added to a round bottom flask. 1,4-Dioxane (30 mL) and aqueous K₃PO₄ (1.35 M, 10 mL) were added and nitrogen bubbled through the mixture for 1 hour. Then, Pd₂(dba)₃ (0.038 g, 0.041 mmol) and 2-dicyclohexylphosphino-2',6'-dimethoxybiphenyl (S-Phos) (0.035 g, 0.083 mmol) were added and the resultant mixture was vigorously stirred for 12 hours at reflux temperature under N₂ flow. The precipitate was filtered, and washed with water and methanol. The resulting pale-yellow solid was purified by chromatography on silica gel (eluent: CHCl₃/Hexane) to afford 6,6'-BPyPh (1.21 g, 98%) as a pale yellow solid. TLC analysis, *R_f*: 0.95 (eluent: chloroform/methanol = 20:1 v/v). ¹H NMR (400 MHz, Chloroform-d) δ = 8.68 (dd, *J* = 7.6, 0.8 Hz, 2H), 8.36 (d, *J* = 1.8 Hz, 4H), 7.98 (t, *J* = 7.9 Hz, 2H), 7.94–7.86 (m, 4H), 7.80–7.74 (m, 8H), 7.56–7.49 (m, 8H), 7.47–7.38 (m, 4H) ppm; EI-MS: *m/z* 612 [*M*]⁺. Anal calcd for C₄₆H₃₂N₂: C, 90.16; H, 5.26; N, 4.57%. Found. C, 90.06; H, 5.25; N, 4.50%.

4,4'-BPy₃, 6,6'-BPy₃, 4,4'-BPh, and 6,6'-BPh were purified by temperature-gradient sublimation in vacuum.

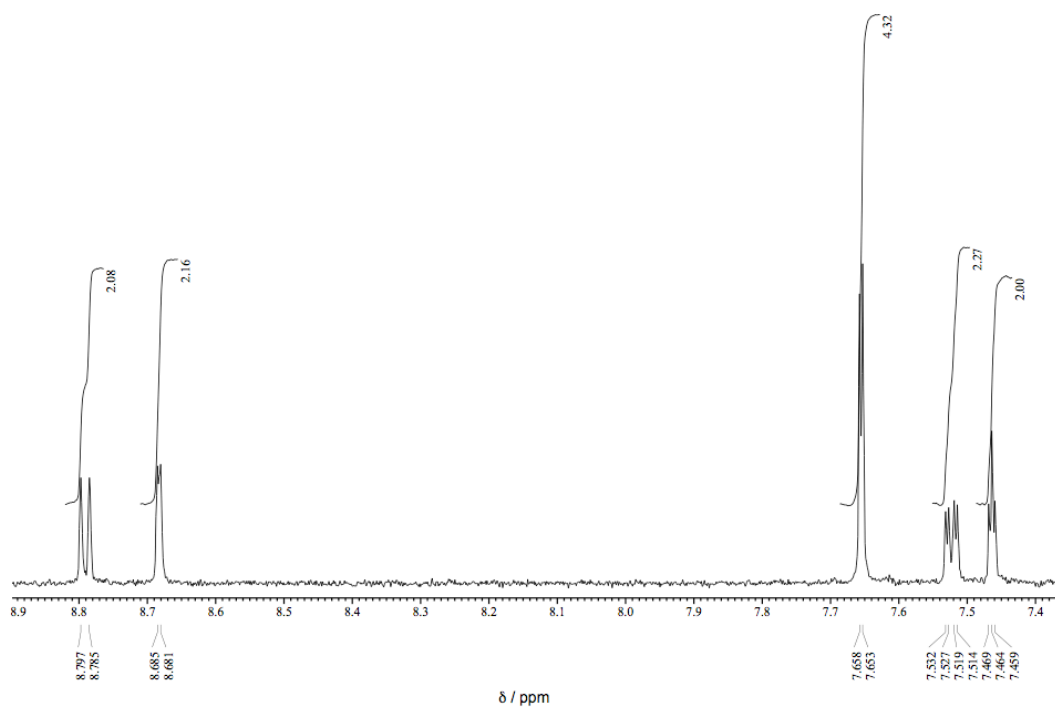
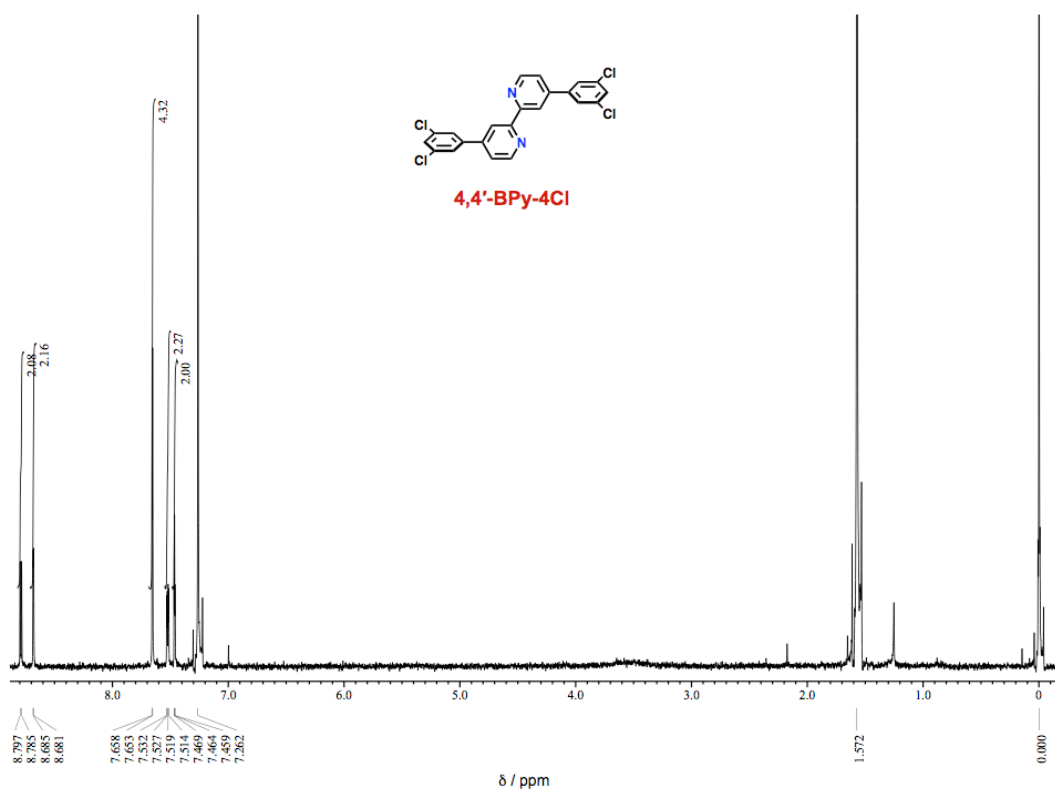


Figure S2. ^1H NMR spectra of 4,4'-BPY-4Cl (400 MHz, CDCl_3).

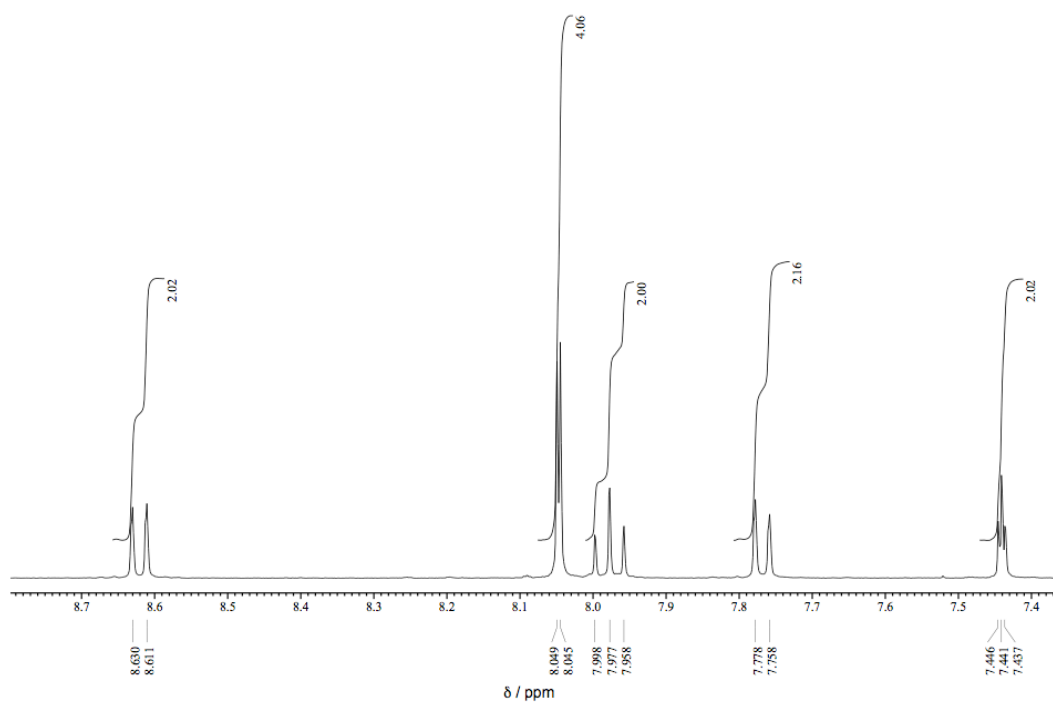
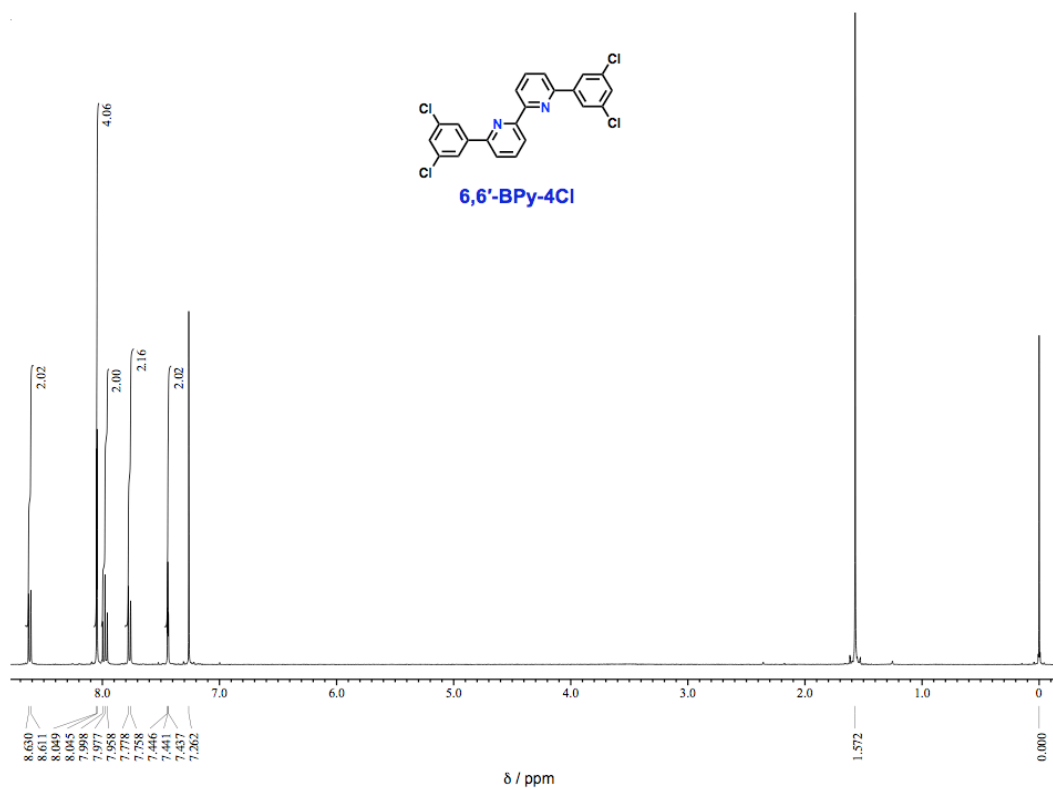


Figure S3. ^1H NMR spectra of 6,6'-BPY-4Cl (400 MHz, CDCl_3).

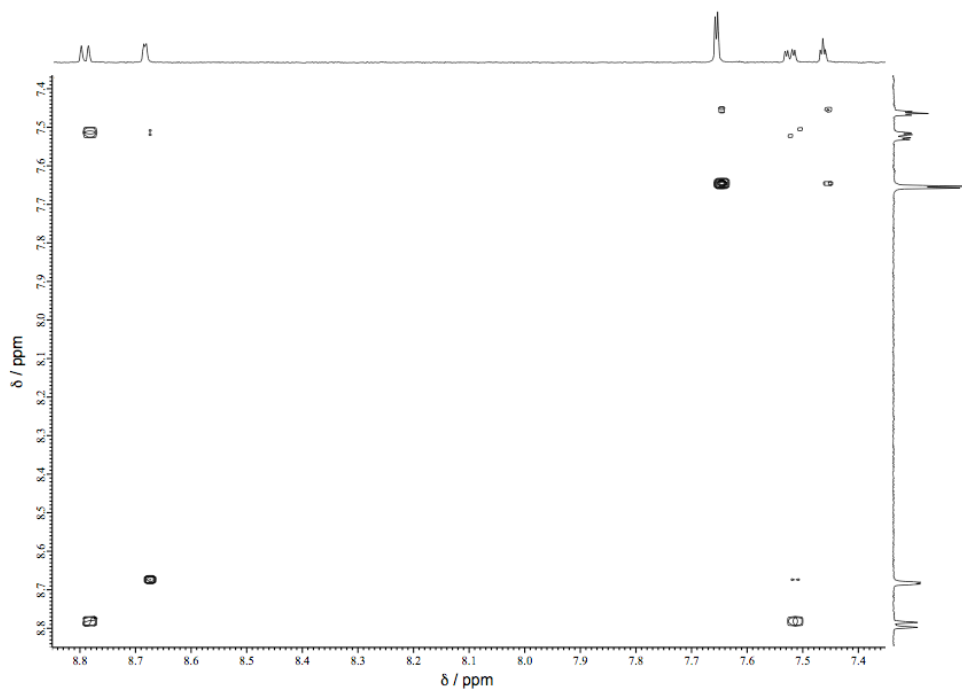


Figure S4. ^1H - ^1H COSY spectrum of 4,4'-BPy-4Cl (400 MHz, CDCl_3).

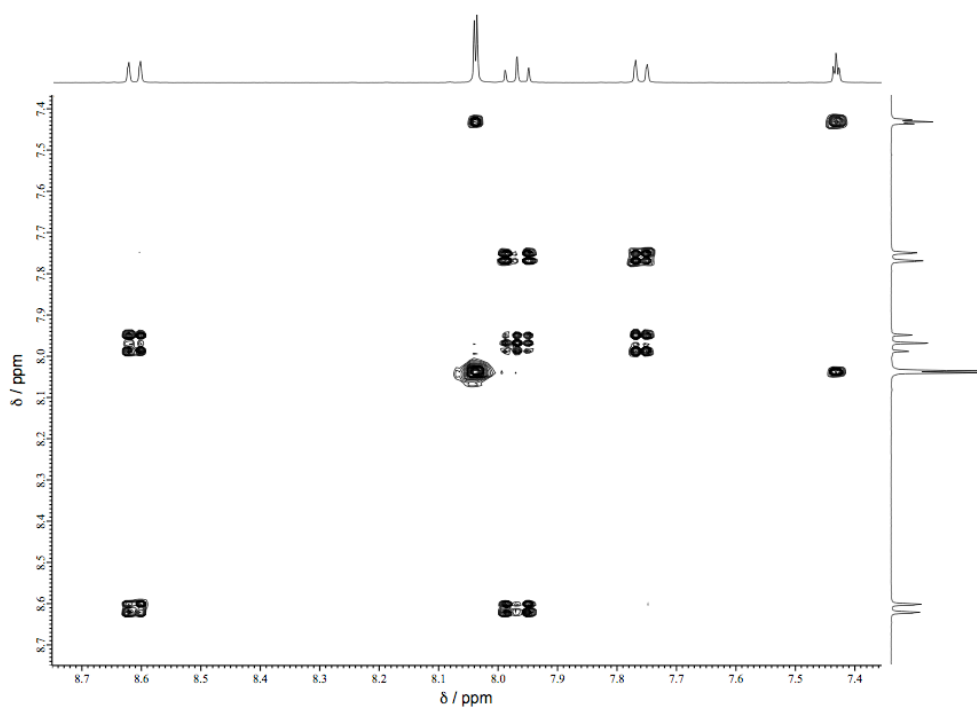


Figure S5. ^1H - ^1H COSY spectrum of 6,6'-BPy-4Cl (400 MHz, CDCl_3).

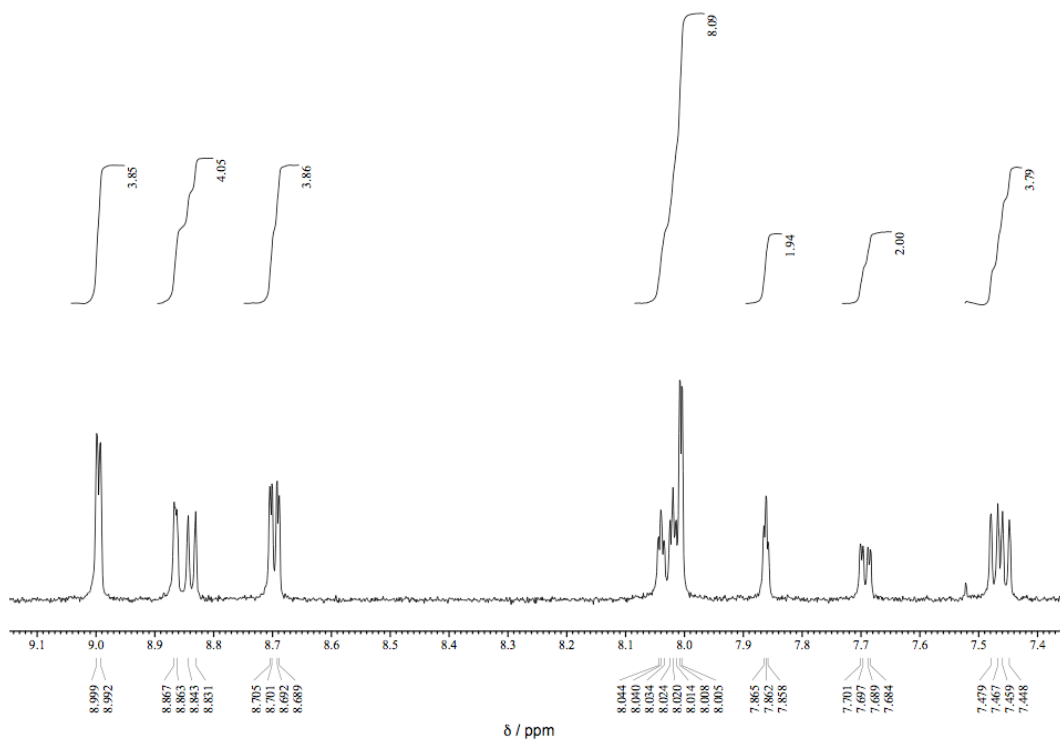
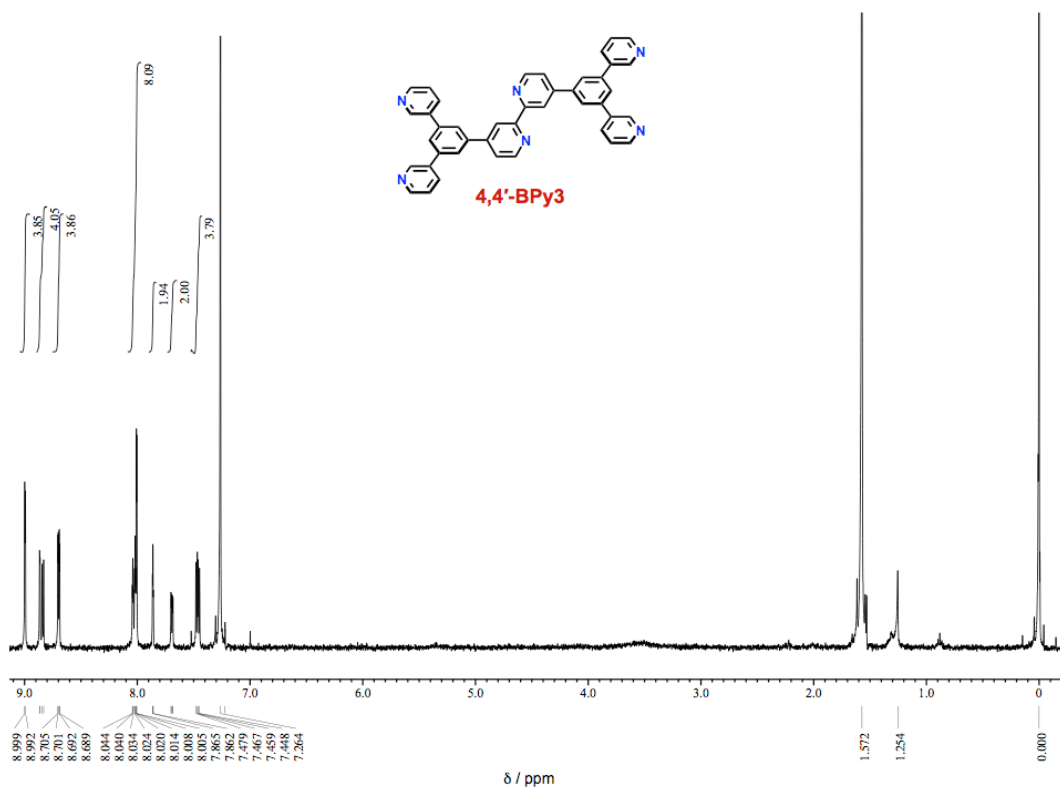


Figure S6. ^1H NMR spectra of 4,4'-BPpy3 (400 MHz, CDCl_3).

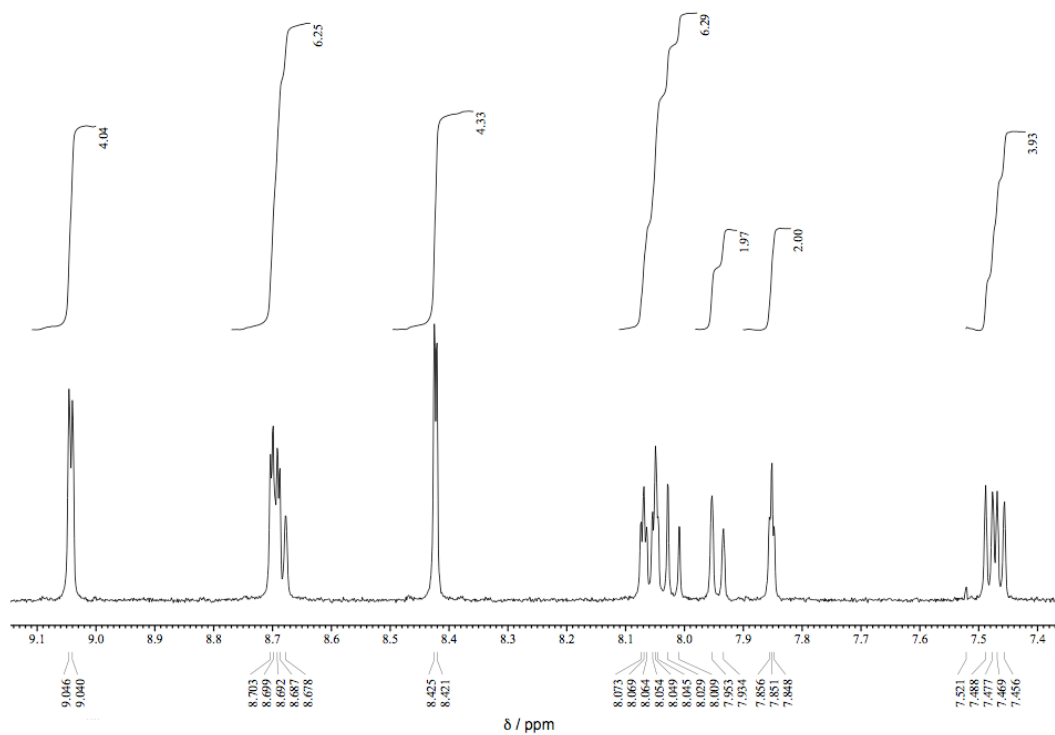
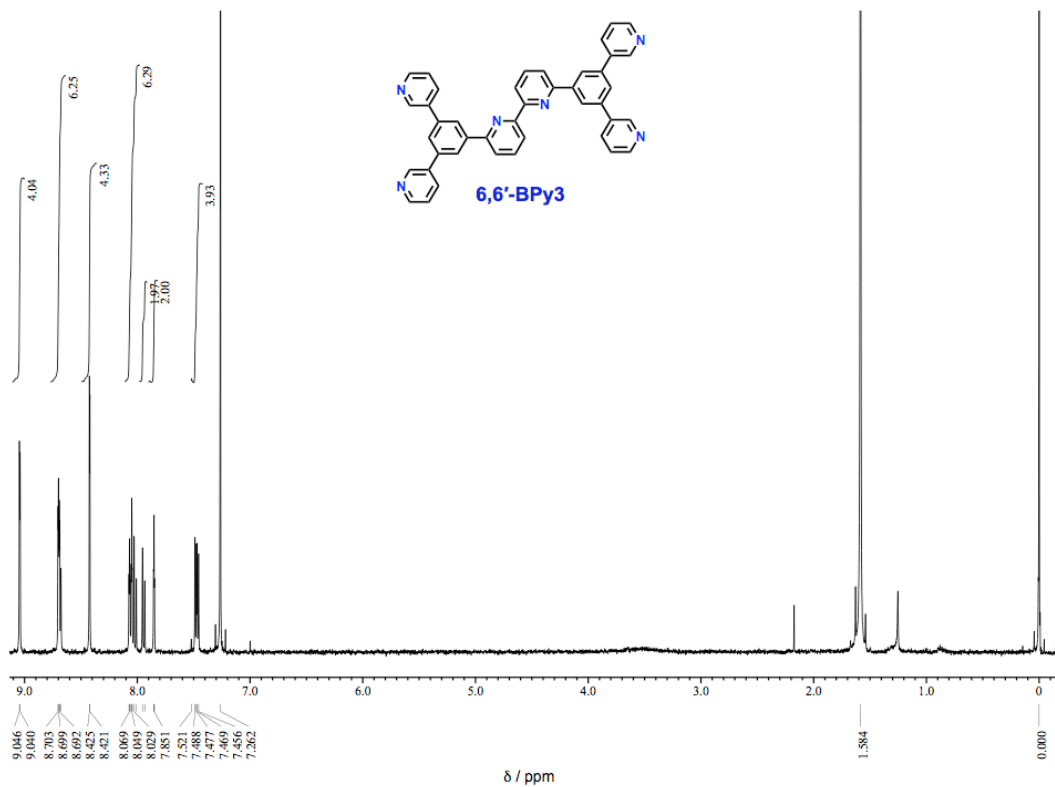


Figure S7. ^1H NMR spectra of 6,6'-BPY3 (400 MHz, CDCl_3).

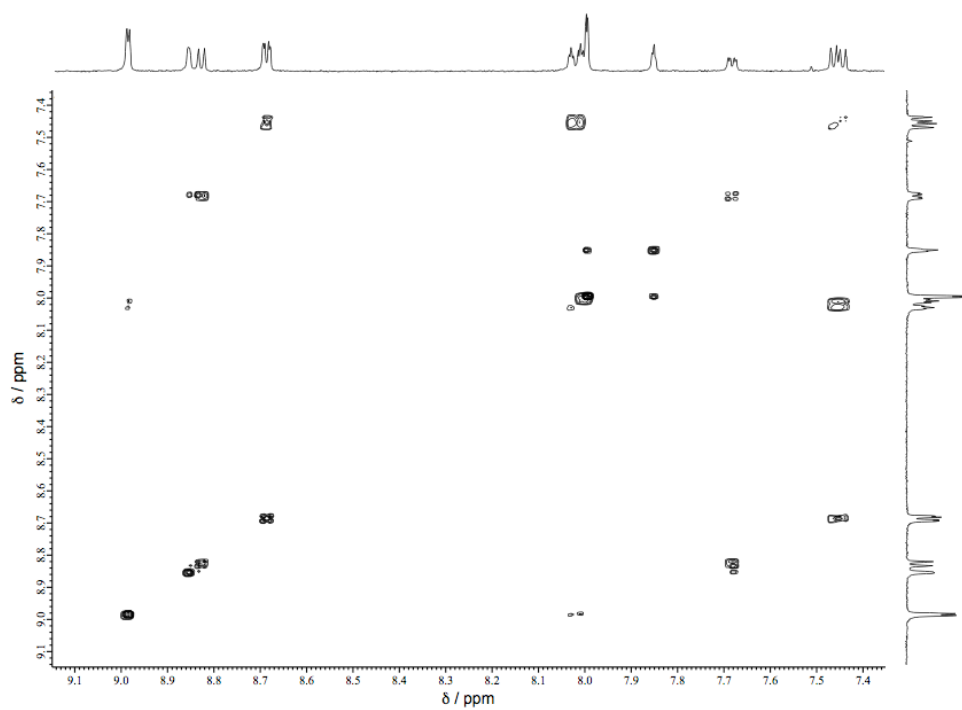


Figure S8. ^1H - ^1H COSY spectrum of 4,4'-BPY3 (400 MHz, CDCl_3).

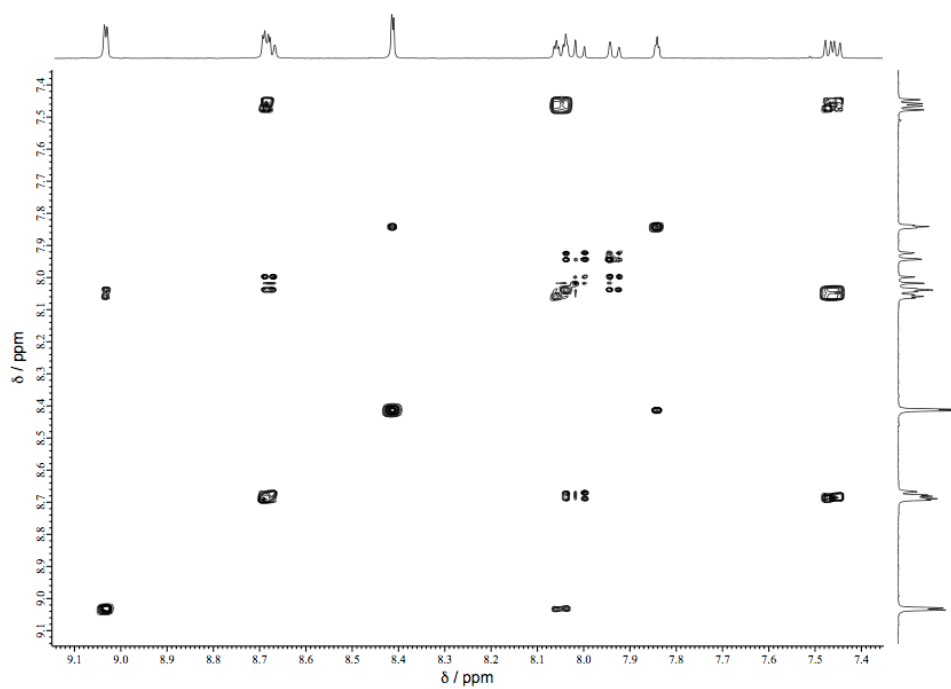


Figure S9. ^1H - ^1H COSY spectrum of 6,6'-BPY3 (400 MHz, CDCl_3).

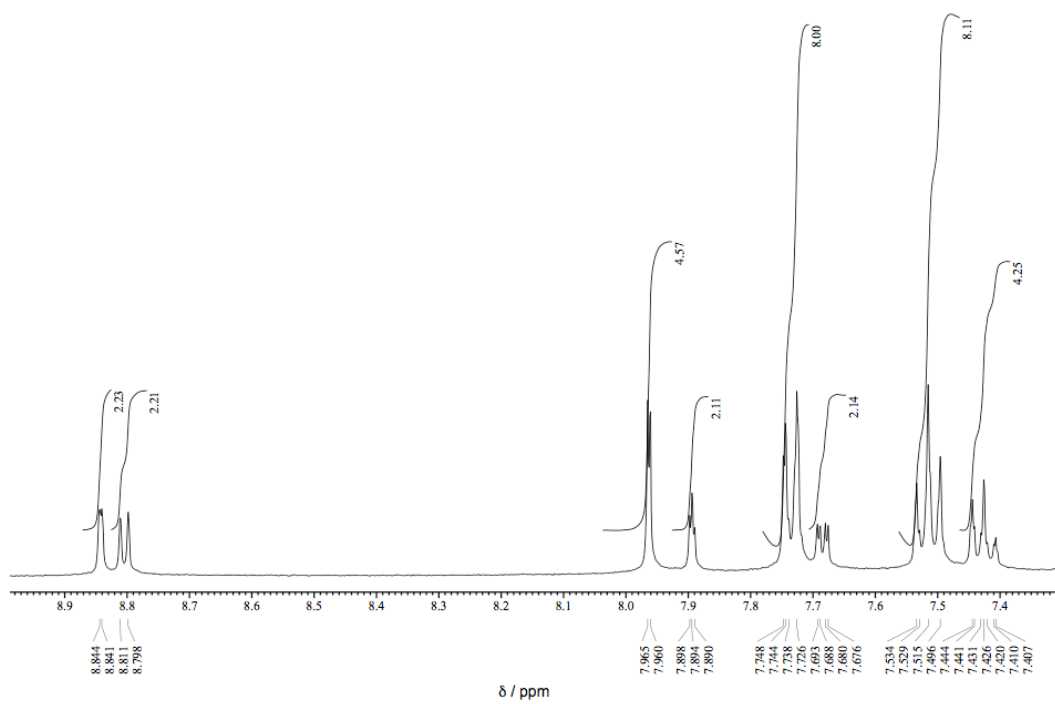
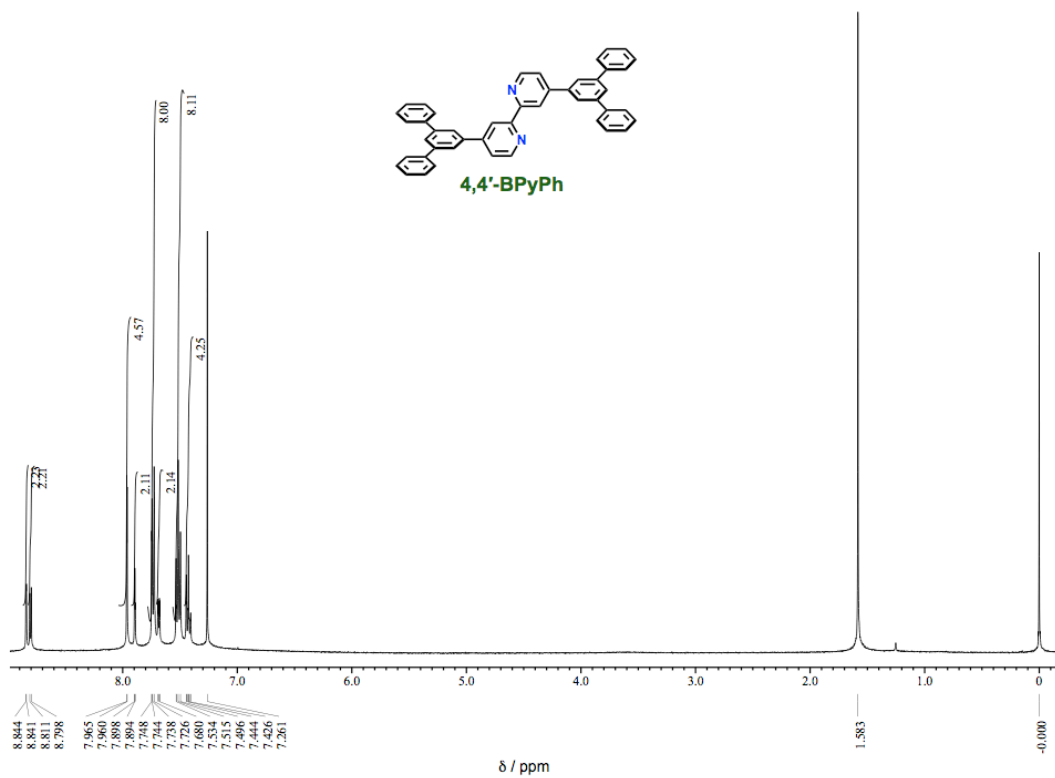


Figure S10. ^1H NMR spectra of 4,4'-BPyPh (400 MHz, CDCl_3).

4. X-ray Crystallographic Structure Determination

4,4'-BPy3

The X-ray diffraction data for 4,4'-BPy3 was collected on a Rigaku Saturn 724 CCD diffractometer with Mo- $K\alpha$ radiation ($\lambda = 0.71075 \text{ \AA}$) at 93 K. Single crystal of 4,4'-BPy3 [$C_{42}H_{28}N_6$, Mw = 616.70] suitable for X-ray analysis were grown by slow gradient sublimation, and a colourless crystal with dimensions $0.20 \times 0.20 \times 0.10 \text{ mm}^3$ was selected for intensity measurements. The unit cell was monoclinic with the space group $P 2_1/c$. Lattice constants with $Z = 2$, $\rho_{\text{calcd}} = 1.386 \text{ g cm}^{-3}$, $\mu = 0.084 \text{ mm}^{-1}$, $F(000) = 644$, and $2\theta_{\text{max}} = 50.48^\circ$ were $a = 3.7736(2)$, $b = 18.7721(13) \text{ \AA}$, $c = 20.9421(15) \text{ \AA}$, $\alpha = 90^\circ$, $\beta = 95.267(5)^\circ$, $\gamma = 90^\circ$, and $V = 1477.24(17) \text{ \AA}^3$. A total of 18887 reflections were collected, of which 3364 reflections were independent ($R_{\text{int}} = 0.0225$). Structure was refined to final $R_1 = 0.0439$ for 3364 data [$I > 2\sigma(I)$] with 238 parameters and $wR_2 = 0.1212$ for all data, $GOF = 1.055$, and residual electron density max./min. = 0.387 and $-0.179 \text{ e.\AA}^{-3}$. The ORTEP drawing is shown in **Figure S12**, and the crystal data and structure refinement are listed in **Table S2**. The data collection, cell refinement, and data reduction were conducted using the CrystalClear-SM Expert software^[2]. The structure was solved by direct methods using the program SHELXS-97^[3] and refined by full matrix least squares methods on F^2 using SHELXL-97^[4]. All the materials for publication were prepared using the Yadokari-XG 2009 software^[5]. All non-hydrogen atoms were refined anisotropically. The positions of all hydrogen atoms were calculated geometrically and refined a riding model.

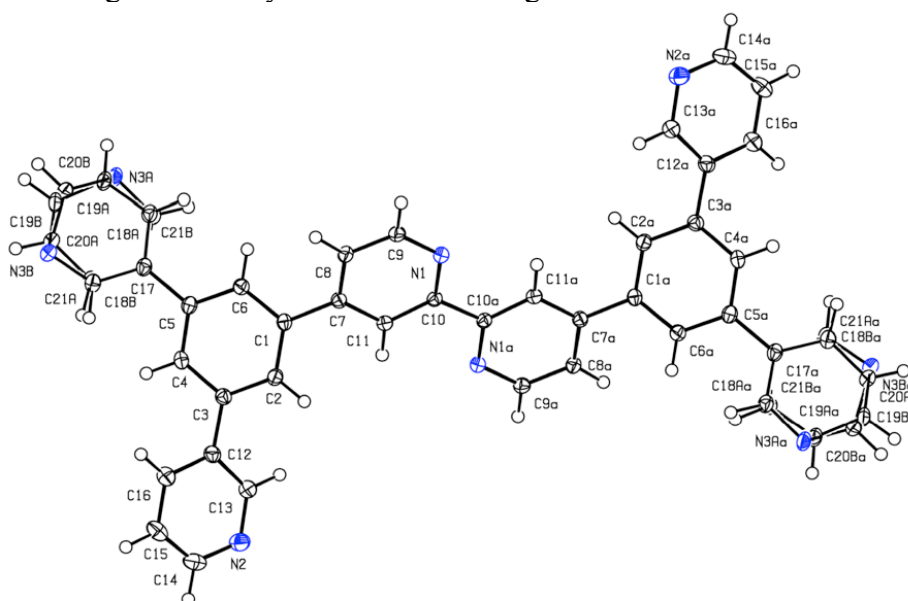


Figure S12. ORTEP diagrams of 4,4'-BPy3 with thermal ellipsoids at 50% probability.

Table S2. Crystal data and structure refinement for 4,4'-BPY3.

Empirical formula	C ₄₂ H ₂₈ N ₆	
Formula weight	616.70	
Temperature	93 K	
Wavelength	0.71075 Å	
Crystal system	Monoclinic	
Space group	<i>P</i> 2 ₁ /c	
Unit cell dimensions	<i>a</i> = 3.7736(2) Å	$\alpha = 90^\circ$
	<i>b</i> = 18.7721(13) Å	$\beta = 95.267(5)^\circ$
	<i>c</i> = 20.9421(15) Å	$\gamma = 90^\circ$
Volume	1477.24(17) Å ³	
Z	2	
Density (calculated)	1.386 g/cm ³	
Absorption coefficient	0.084 mm ⁻¹	
<i>F</i> (000)	644	
Crystal size	0.200 × 0.200 × 0.100 mm ³	
Theta range for data collection	3.125 to 27.494°	
Index ranges	-4 ≤ <i>h</i> ≤ 4, -24 ≤ <i>k</i> ≤ 24, -27 ≤ <i>l</i> ≤ 27	
Reflections collected	18887	
Independent reflections	3364 [<i>R</i> (int) = 0.0225]	
Completeness to theta = 25.242°	99.7 %	
Absorption correction	Semi-empirical from equivalents	
Max. and min. transmission	1.000 and 0.914	
Refinement method	Full-matrix least-squares on <i>F</i> ²	
Data / restraints / parameters	3364 / 16 / 238	
Goodness-of-fit on <i>F</i> ²	1.055	
Final <i>R</i> indices [<i>I</i> > 2σ(<i>I</i>)]	<i>R</i> ₁ = 0.0439, <i>wR</i> ₂ = 0.1182	
<i>R</i> indices (all data)	<i>R</i> ₁ = 0.0480, <i>wR</i> ₂ = 0.1212	
Largest diff. peak and hole	0.387 and -0.179 e.Å ⁻³	

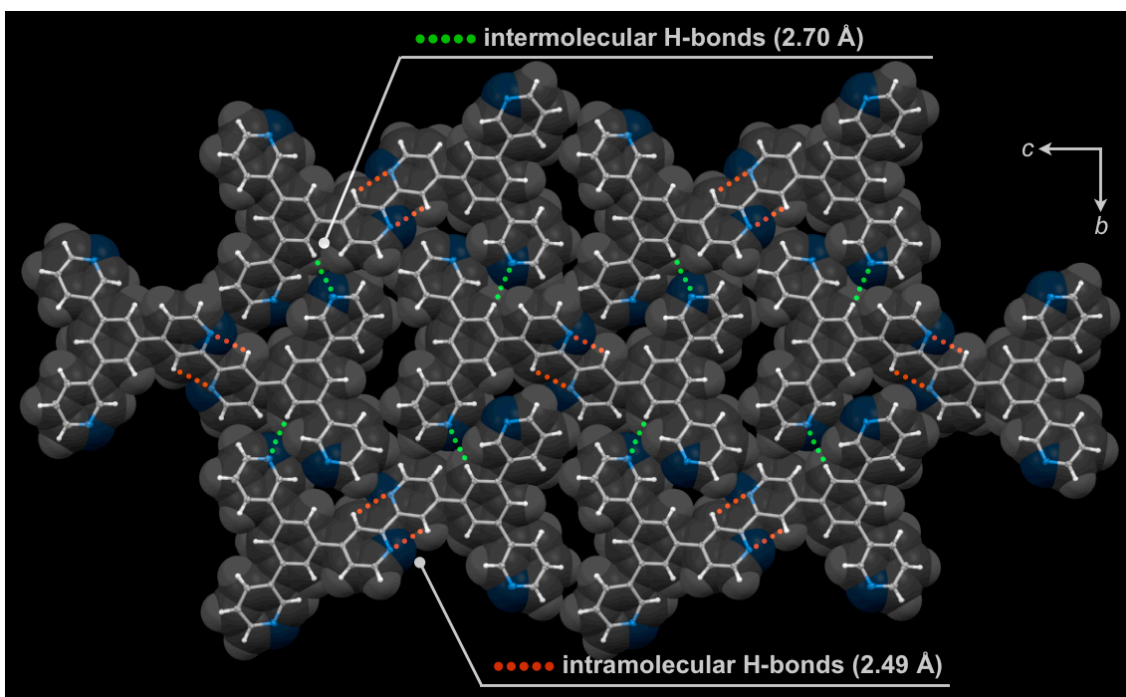


Figure S13. Crystal structures of 4,4'-BPY3: partially cutaway view focused on the intermolecular H-bonding network is illustrated with thermal ellipsoids drawn at the 50% probability level.

6,6'-BPy3

The X-ray diffraction data for 6,6'-BPy3 was collected on a Rigaku Saturn 724 CCD diffractometer with Mo- $K\alpha$ radiation ($\lambda = 0.71075 \text{ \AA}$) at 93 K. Single crystal of 6,6'-BPy3 [$C_{42}H_{28}N_6$, Mw = 616.70] suitable for X-ray analysis were grown by slow gradient sublimation, and a colourless crystal with dimensions $0.33 \times 0.13 \times 0.10 \text{ mm}^3$ was selected for intensity measurements. The unit cell was monoclinic with the space group $C 2/c$. Lattice constants with $Z = 4$, $\rho_{\text{calcd}} = 1.357 \text{ g cm}^{-3}$, $\mu = 0.082 \text{ mm}^{-1}$, $F(000) = 1288$, and $2\theta_{\text{max}} = 50.48^\circ$ were $a = 32.776(12)$, $b = 3.8953(14) \text{ \AA}$, $c = 23.750(9) \text{ \AA}$, $\alpha = 90^\circ$, $\beta = 95.426(5)^\circ$, $\gamma = 90^\circ$, and $V = 3018.6(19) \text{ \AA}^3$. A total of 18153 reflections were collected, of which 3437 reflections were independent ($R_{\text{int}} = 0.0302$). Structure was refined to final $R_1 = 0.0505$ for 3437 data [$I > 2\sigma(I)$] with 235 parameters and $wR_2 = 0.1316$ for all data, $GOF = 1.083$, and residual electron density max./min. = 0.323 and $-0.292 \text{ e.\AA}^{-3}$. The ORTEP drawing is shown in **Figure S13**, and the crystal data and structure refinement are listed in **Table S3**. The data collection, cell refinement, and data reduction were conducted using the CrystalClear-SM Expert software^[2]. The structure was solved by direct methods using the program SHELXS-97^[3] and refined by full matrix least squares methods on F^2 using SHELXL-97^[4]. All the materials for publication were prepared using the Yadokari-XG 2009 software^[5]. All non-hydrogen atoms were refined anisotropically. The positions of all hydrogen atoms were calculated geometrically and refined a riding model.

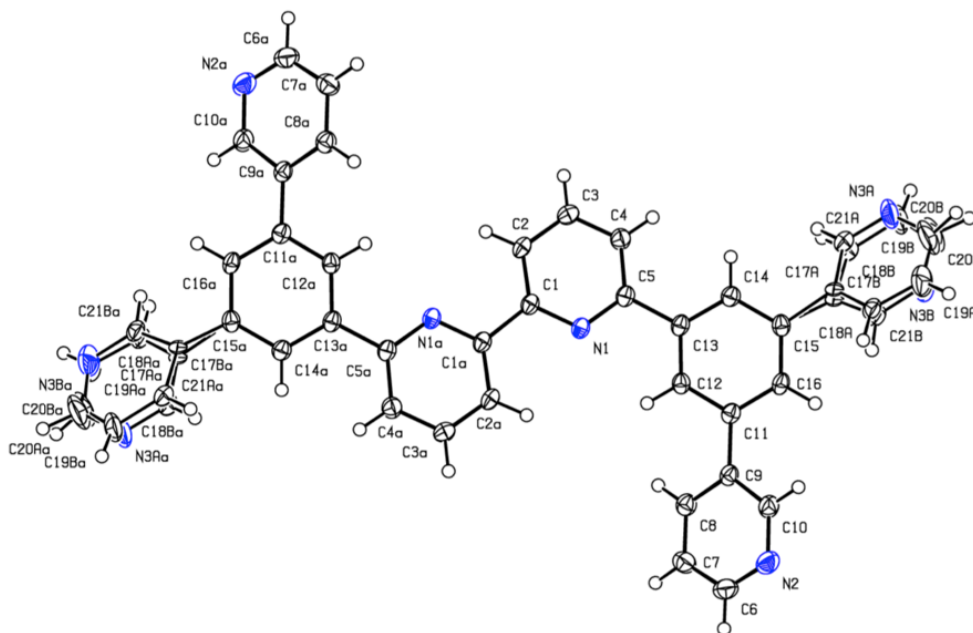


Figure S14. ORTEP diagrams of 6,6'-BPy3 with thermal ellipsoids at 50% probability.

Table S3. Crystal data and structure refinement for 6,6'-BPY3.

Empirical formula	C ₄₂ H ₂₈ N ₆	
Formula weight	616.70	
Temperature	93 K	
Wavelength	0.71075 Å	
Crystal system	Monoclinic	
Space group	<i>C</i> 2/c	
Unit cell dimensions	$a = 32.776(12)$ Å	$\alpha = 90^\circ$
	$b = 3.8953(14)$ Å	$\beta = 95.426(5)^\circ$
	$c = 23.750(9)$ Å	$\gamma = 90^\circ$
Volume	3018.6(19) Å ³	
Z	4	
Density (calculated)	1.357 g/cm ³	
Absorption coefficient	0.082 mm ⁻¹	
<i>F</i> (000)	1288	
Crystal size	0.330 × 0.130 × 0.100 mm ³	
Theta range for data collection	3.447 to 27.496°	
Index ranges	-42 ≤ <i>h</i> ≤ 42, -5 ≤ <i>k</i> ≤ 5, -30 ≤ <i>l</i> ≤ 30	
Reflections collected	18153	
Independent reflections	3437 [<i>R</i> (int) = 0.0302]	
Completeness to theta = 25.242°	99.7 %	
Absorption correction	Semi-empirical from equivalents	
Max. and min. transmission	1.000 and 0.903	
Refinement method	Full-matrix least-squares on <i>F</i> ²	
Data / restraints / parameters	3437 / 16 / 235	
Goodness-of-fit on <i>F</i> ²	1.083	
Final <i>R</i> indices [<i>I</i> > 2σ(<i>I</i>)]	<i>R</i> ₁ = 0.0505, <i>wR</i> ₂ = 0.1237	
<i>R</i> indices (all data)	<i>R</i> ₁ = 0.0601, <i>wR</i> ₂ = 0.1316	
Largest diff. peak and hole	0.323 and -0.292 e.Å ⁻³	

5. Thermal Properties

Table S4. Thermal properties of BPy and BPyPh derivatives.

Compound	Mw	T_g^a (°C)	T_c^a (°C)	T_m^a (°C)	T_{d5}^b (°C)
4,4'-BPyPh	613	N.d.	164	289	462
6,6'-BPyPh	613	N.d.	163	259	455
4,4'-BPy3	617	N.d.	N.d.	352	490
6,6'-BPy3	617	N.d.	N.d.	341	455

^{a)} T_g and T_m were measured by differential scanning calorimetry (DSC). ^{b)} T_{d5} was measured by thermogravimetric analysis (TGA).

6. Optical properties

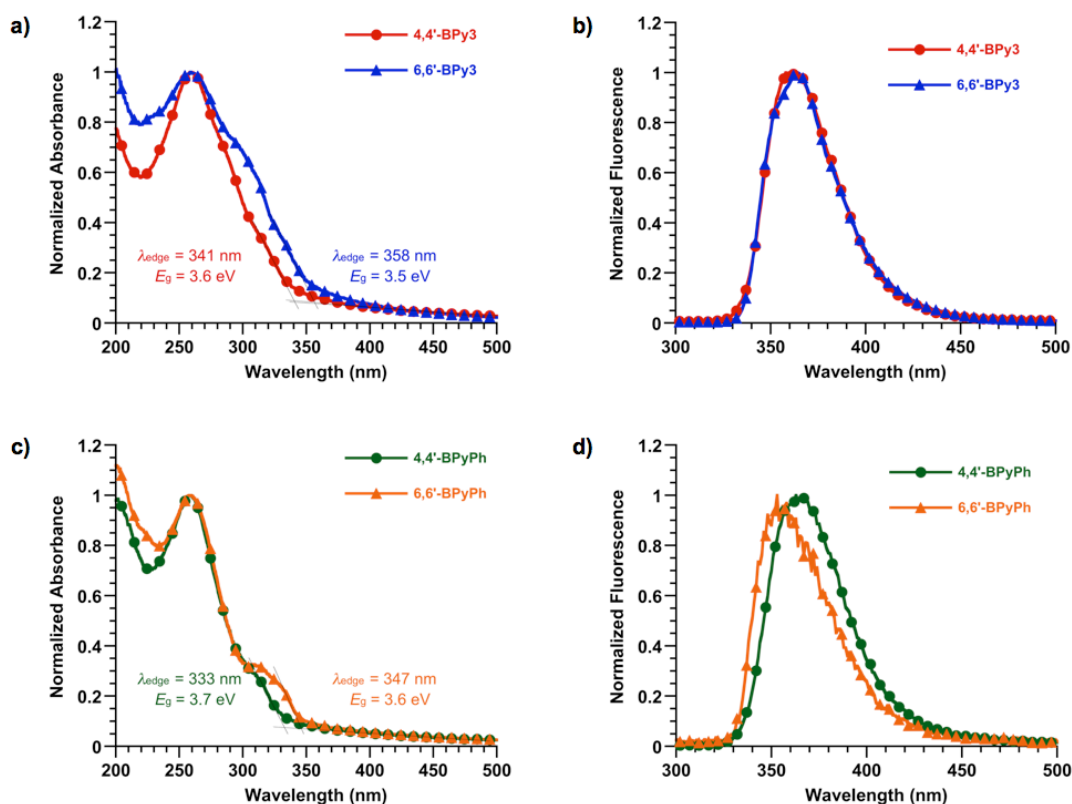


Figure S15. UV-vis, PL spectra of BPy derivatives: a) and b) BPy derivatives; c) and d) BPyPh derivatives films, respectively.

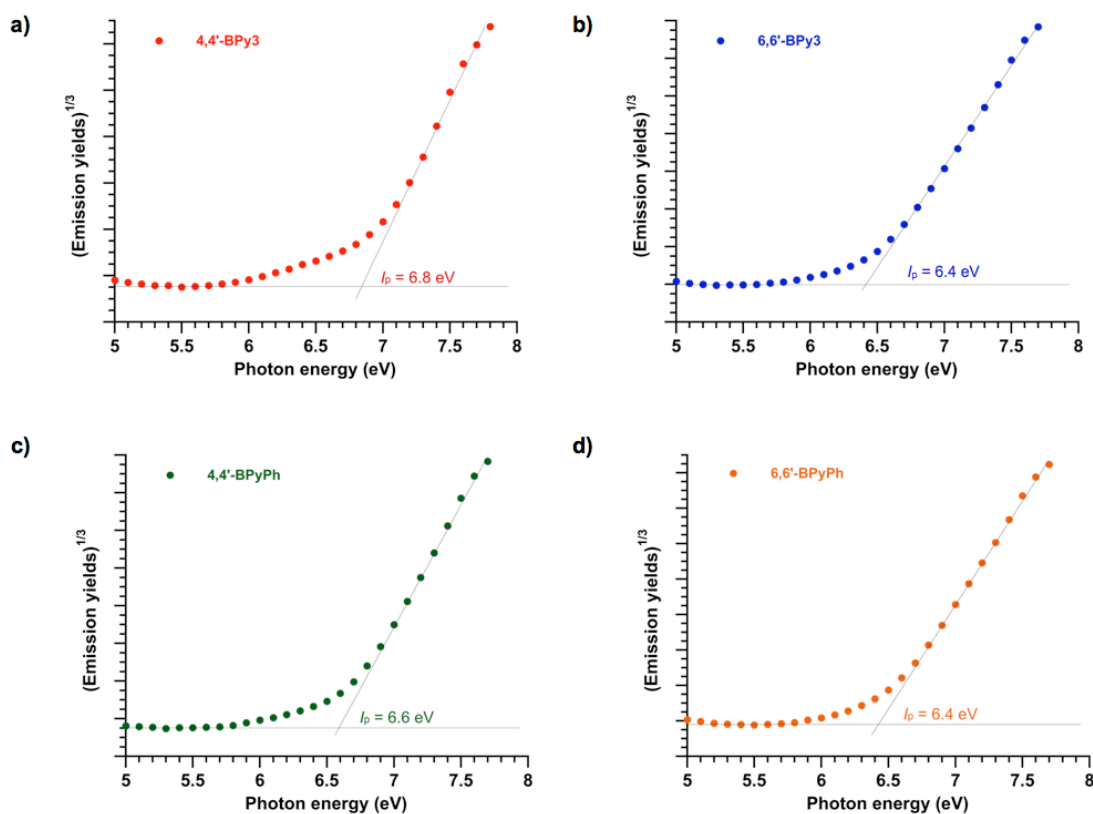


Figure S16. Photoelectron yield spectroscopy (PYS) spectra of BPy derivatives: a) and b) BPy derivatives; c) and d) BPyPh derivatives films, respectively.

Table S5. Electronic properties of BPy and BPyPh derivatives.

Compound	λ_{\max} ^{a)} (nm)	I_p ^{b)} (eV)	E_g ^{c)} (eV)	E_a ^{d)} (eV)
4,4'-BPyPh	363	-6.6	3.7	-2.9
6,6'-BPyPh	353	-6.4	3.6	-2.8
4,4'-BPy3	362	-6.8	3.6	-3.2
6,6'-BPy3	364	-6.4	3.5	-3.0

^{a)} $\lambda_{\text{ex}} = 260$ nm. ^{b)} I_p was measured by photoelectron yield spectroscopy (PYS). ^{c)}The E_g was taken as the point of intersection of the normalized absorption spectra. ^{d)} E_a was calculated using I_p and E_g .

7. Time of Flight measurements

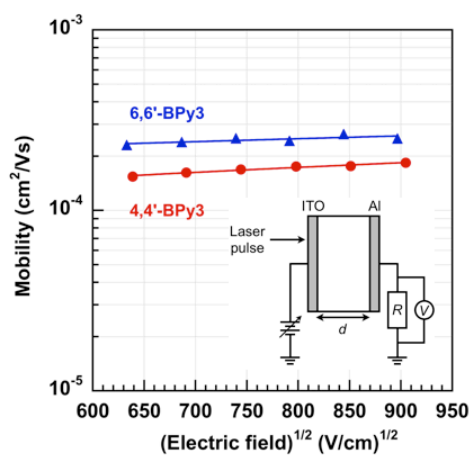


Figure S17. Dependences of electron motilities of 4,4'-BPy3 and 6,6'-BPy3 films on electric field obtained by TOF measurements at 298 K.

8. Electron Only Devices

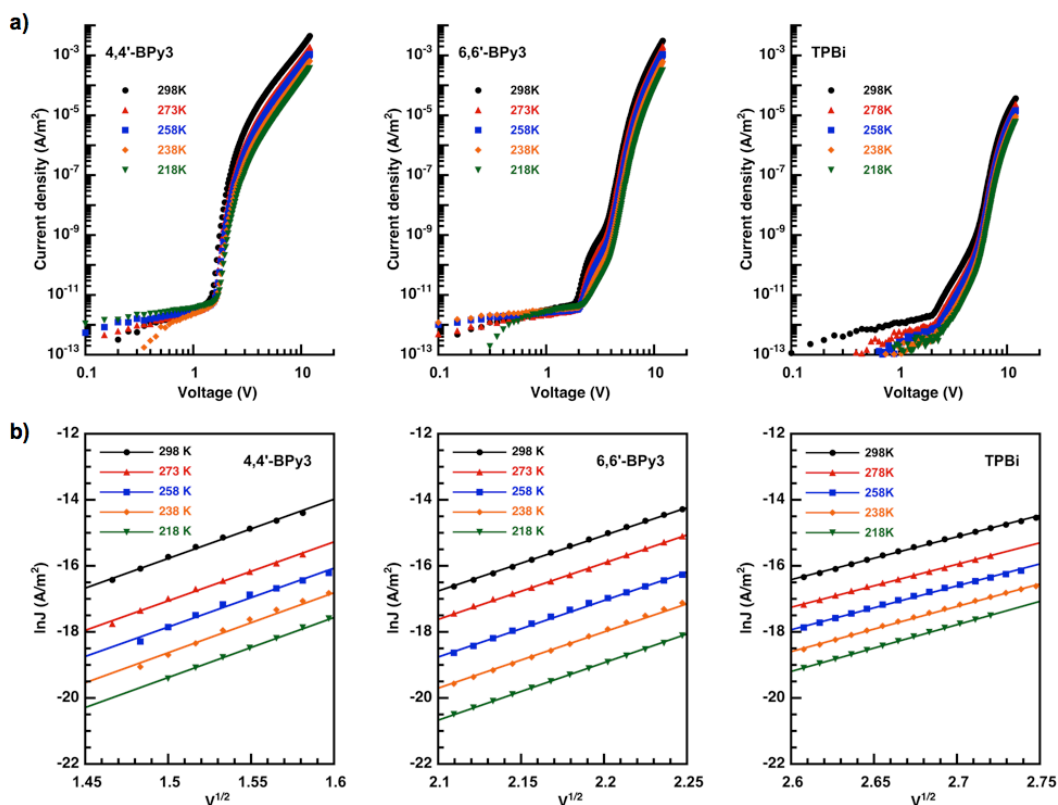
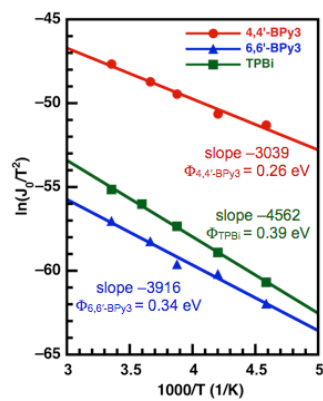


Figure S18. Electron injection properties into ETL layer from Al cathode. The electron only device of ITO/ETL (200 nm) /Liq(3 nm) /Al(100 nm)(ETL= 4,4'-BPy3, 6,6'-BPy3 and TPBi) were fabricated. a) Temperature dependence of current density (J) versus the voltage (V); b) Relationship between $\ln J$ and $V^{1/2}$ characteristics.



$$J = A^* T^2 \exp \left[\frac{-q(\Phi - \sqrt{qV / 4\pi\epsilon})}{kT} \right] \quad (1)$$

$$J_0 = A^* T^2 \exp^{-q\Phi/kT} \quad (2)$$

$$\ln \left(\frac{J_0}{T^2} \right) = - \left(\frac{q\Phi_b}{k} \right) \frac{1}{T} + \ln A^* \quad (3)$$

A^* : Richardson constant
 T : temperature
 q : electronic charge
 V : applied voltage
 Φ : barrier height at the interface

Figure S19. Relationship between $\ln J_0/T^2$ and $1/T$. The V_0 values were obtained by extrapolating the each lines in **Figure S17** to $V=0$.

9. OLEDs

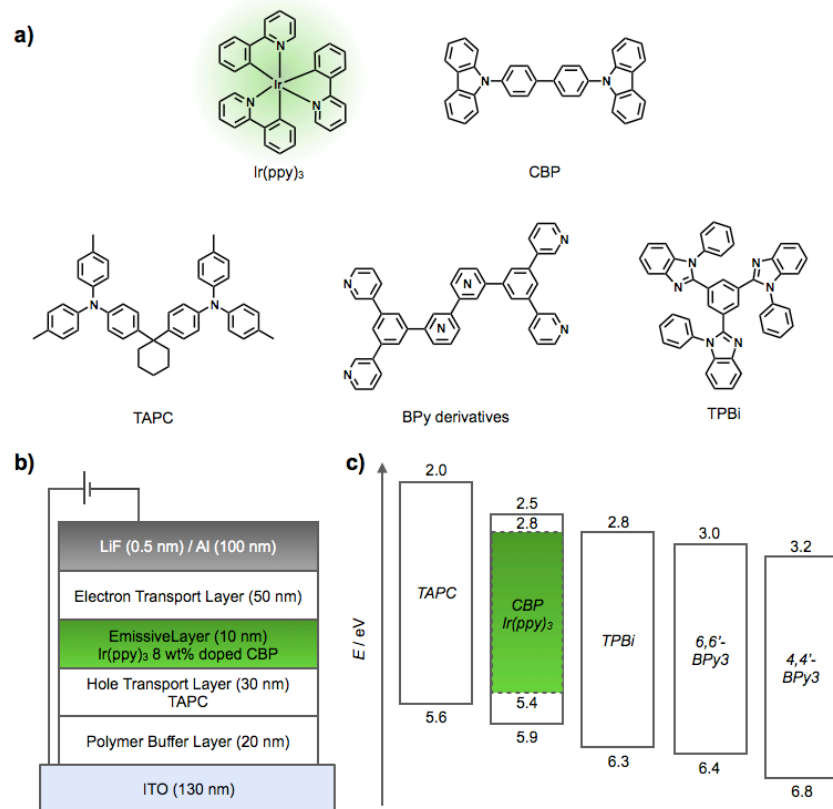


Figure S20. a) Chemical structures, b) device structure, and c) energy diagram of devices.

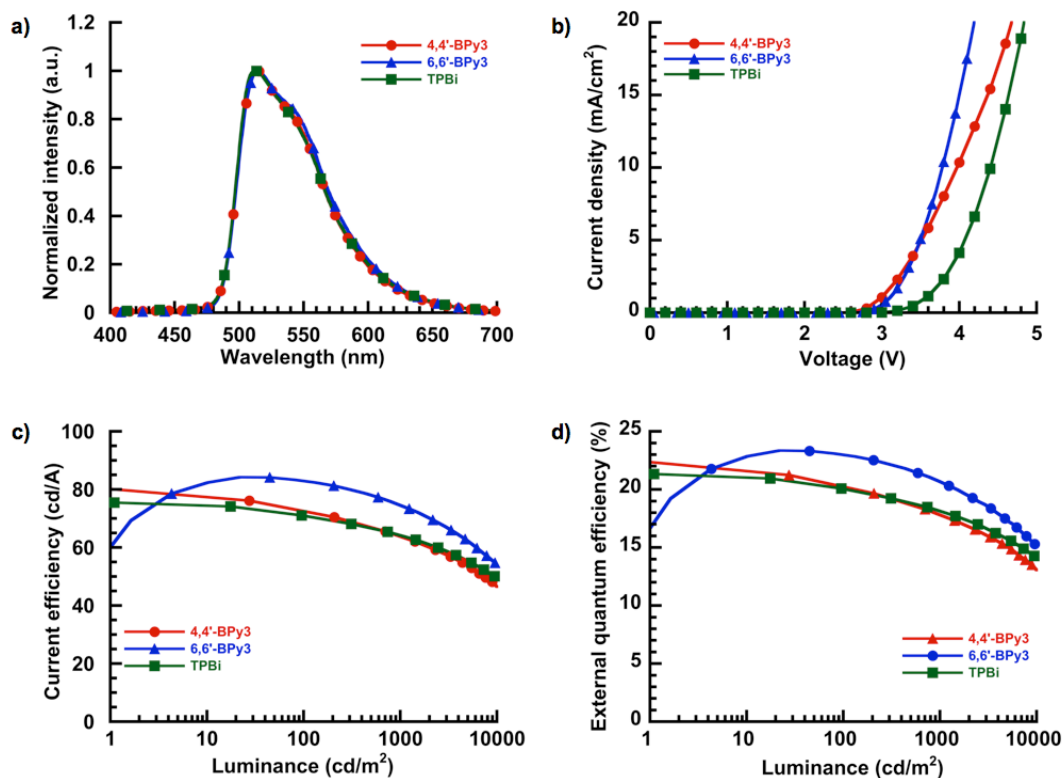


Figure S21. a) EL spectra at 1 mA, b) Current density–voltage characteristics, c) current efficiency–luminance characteristics, and d) external quantum efficiency–luminance characteristics.

Table S6. Performance of OLEDs with a device structure of [ITO (130 nm)/ triphenylamine-containing polymer: PPBI (20 nm)/TAPC (30 nm)/8 wt% Ir(ppy)₃-doped CBP (10 nm)/ETL (50 nm)/LiF (0.5 nm)/Al (100 nm)].

ETM	V_{on} ^{a)} [V]	$V_{100}/\eta_{\text{p},100}/\eta_{\text{c},100}/\eta_{\text{ext},100}$ ^{b)} [V/lm W ⁻¹ /cd A ⁻¹ /%]	$V_{1000}/\eta_{\text{p},1000}/\eta_{\text{c},1000}/\eta_{\text{ext},1000}$ ^{c)} [V/lm W ⁻¹ /cd A ⁻¹ /%]
4,4'-BPy3	2.40	2.68/86.8/73.8/20.6	3.08/65.4/64.1/17.9
6,6'-BPy3	2.52	2.82/92.4/82.9/23.0	3.15/74.3/74.6/20.7
TPBi	2.78	3.20/69.6/71.0/20.1	3.67/55.2/64.4/18.2

a) Voltage (V) at 1 cd m⁻². b) Power efficiency (η_{p}), current efficiency (η_{c}), and external quantum efficiency (η_{ext}) at 100 cd m⁻². c) V , η_{p} , η_{c} , and η_{ext} at 1000 cd m⁻².

10. References

- [1] *Gaussian 09*, Revision D.01, M. J. Frisch, G. W. Trucks, H. B. Schlegel, G. E. Scuseria, M. A. Robb, J. R. Cheeseman, G. Scalmani, V. Barone, B. Mennucci, G. A. Petersson, H. Nakatsuji, M. Caricato, X. Li, H. P. Hratchian, A. F. Izmaylov, J. Bloino, G. Zheng, J. L. Sonnenberg, M. Hada, M. Ehara, K. Toyota, R. Fukuda, J. Hasegawa, M. Ishida, T. Nakajima, Y. Honda, O. Kitao, H. Nakai, T. Vreven, J. A. Montgomery, Jr., J. E. Peralta, F. Ogliaro, M. Bearpark, J. J. Heyd, E. Brothers, K. N. Kudin, V. N. Staroverov, R. Kobayashi, J. Normand, K. Raghavachari, A. Rendell, J. C. Burant, S. S. Iyengar, J. Tomasi, M. Cossi, N. Rega, J. M. Millam, M. Klene, J. E. Knox, J. B. Cross, V. Bakken, C. Adamo, J. Jaramillo, R. Gomperts, R. E. Stratmann, O. Yazyev, A. J. Austin, R. Cammi, C. Pomelli, J. W. Ochterski, R. L. Martin, K. Morokuma, V. G. Zakrzewski, G. A. Voth, P. Salvador, J. J. Dannenberg, S. Dapprich, A. D. Daniels, Ö. Farkas, J. B. Foresman, J. V. Ortiz, J. Cioslowski, and D. J. Fox, Gaussian, Inc., Wallingford CT, **2013**.
- [2] CrystalClear-SM Expert: Rigaku Corporation, Tokyo, Japan, **2011**.
- [3] SHELXS"97: Sheldrick, G. M. Program for the Solution of Crystal Structures; *Acta Crystallogr. A* **2008**, *64*, 112–122.
- [4] SHELXL"97: Sheldrick, G. M. Program for the Refinement of Crystal Structures; *Acta Crystallogr. A* **2008**, *64*, 112–122.
- [5] a) Yadokari"XG: Wakita, K. Software for crystal Structure Analyses, **2001**; b) Yadokari"XG**2009**: C. Kabuto, S. Akine, T. Nemoto, E. Kwon. Release of Software for Crystal Structure Analyses; *J. Cryst. Soc. Jpn.* **2009**, *51*, 218–224.